

Depth of Cut Monitoring for Hybrid Manufacturing Using Acoustic Emission Sensor

Haythem Gaja*, Frank Liou*⁺

* Mechanical Engineering Missouri University of Science and Technology, Rolla, MO 65409

REVIEWED

Abstract

Laser Metal Deposition LMD is a hybrid manufacturing process consist of a laser deposition system combined with a 5-axis CNC milling system. During laser deposition many parameters and their interaction affect the dimensional accuracy of the part produced, powder flow rate, laser power and travel speed are some of these parameters. Sensing the acoustic emission during milling marching gives feedback information regarding depth of metal being cut subsequent part dimensions, if an error in dimensions is found certain actions, such as remaching, close loop control, or laser remelting can be carried out to correct it. Thus a reliable hybrid manufacturing management system requires that a depth-of-cut detection system be integrated with the milling machine architecture. This work establishes, first a methodology to detect an acoustic emission signal, so that the acoustic emission characteristics of the milling could be analyzed. Second, it sought to relate these acoustic data to machining parameters to detect depth-of-cut.

Keywords: Depth of cut Detection, Acoustic emission, artificial neural network

INTRODUCTION

One of the difficulties in using an adaptive control and tool monitoring system is accurate representation of the variation in machining variables such as cutting speed, feed rate, and depth-of-cut. In the end-milling process, particular changes in depth-of-cut must be carefully considered to ensure the effectiveness of the control system.

Many researchers have sought to control surface errors and radial and axial depth-of-cut using analytical models, simulation, force sensors, and other sensors. Choi [1] suggested an algorithm to estimate the cutting depth based on the pattern of cutting force. He found that the cutting force pattern is more useful for this purpose than its magnitude because its pattern reflects the change in cutting depth. However, magnitude is affected by a number of cutting variables, but not by the depth-of-cut.

Yang [2] suggested an analytical method to identify depth-of-cut variations based on cutting force profile features detected during end milling. Based on the profile characteristics of a single-flute, he studied end mill cutting forces and categorized them into three types. The same study categorized the cutting forces signals of both the single-flute end mill cutting and the multiple-flute end mill cutting based on the cutting process.

Wan [3] predicted the cutting forces and the surface dimensional errors using iteration schemes. Using the finite element method, he devolved a general method to calculate static form errors in peripheral milling of thin-walled structures, and his simulation tool considered the complexity of the workpiece.

Li [4] presented a comprehensive time domain model for general end milling processes. The model measures variations in depth-of-cut using mode forms. The model can also consider additional general conditions such as cutting with a large axial depth-of-cut or small discontinued radial depth-of-cut. In addition to simulating the end milling process this method predicts a number of results for surface profiles and chatter boundaries.

Yonggang [5] examined cutting forces and categorized them into six classes according to a combination of cutting depths, and he proposed a finite-element model to study surface dimensional errors in peripheral milling of thin-walled workpieces for aerospace application. Such error prediction keeps the number of surface errors within permissible bounds.

To forecast a surface form error with the greatest efficiency and accuracy, Yonggang's model relies on a set of flexible iterative rules with a double iterative algorithm. Prickett [6] presented an approach that uses ultrasonic sensors for online monitoring of depth-of-cut during the end milling processes. The proposed monitoring process tried to contribute to the development of more efficient tool management procedures and supporting infrastructure. However, sensor resolution is an important factor limiting performance.

This work used a fitting model with a Neural Network to represent the relationship between the acoustic emission signal and depth-of-cut. The output of the sensor and data of cutting conditions and tool status are fed to a neural network to measure operation quality during machining. After the network was trained, the inference system estimated the depth-of-cut in real time from the experimental sensor signal and the cutting conditions. The results of the monitoring algorithm can warn the operator to take the corrective actions to reach the required depth-of-cut. The difference between the desired depth-of-cut and the actual depth-of-cut may be a result of incorrect workpiece set-up, tool length offset change (tool wear), or irregularity of workpiece dimensions. Previous manufacturing processes may also lead to errors in depth-of-cut. For example, when a workpiece is manufactured by laser deposition, forging, or casting, the dimensions are not always accurate and uniform.

EXPERIMENTAL SETUP

Figure 1 shows a schematic diagram of the experimental set-up. The milling process was carried out on a Fadal vertical 5-Axis computer numerical control machine (3016L) using a carbide flat-end mill (0.5 in) to cut deposited stainless steel 316 workpieces. The control interface (National Instrument PXI 7240 and PXI 1250) provided the control and data acquisition. An acoustic emission sensor (Kistler 8152B211) captured a high-frequency signal. The bandwidth of the AE sensor was 10 to 1000 kHz. The RMS signals were first fed through the data acquisition system and then recoded and processed using Labview software. A 500X digital microscopic

camera was used to detect tool status without disengaging the tool from the tool holder. The tool condition was documented from the bottom edge radius, which was measured in place with the aid of the vision system.

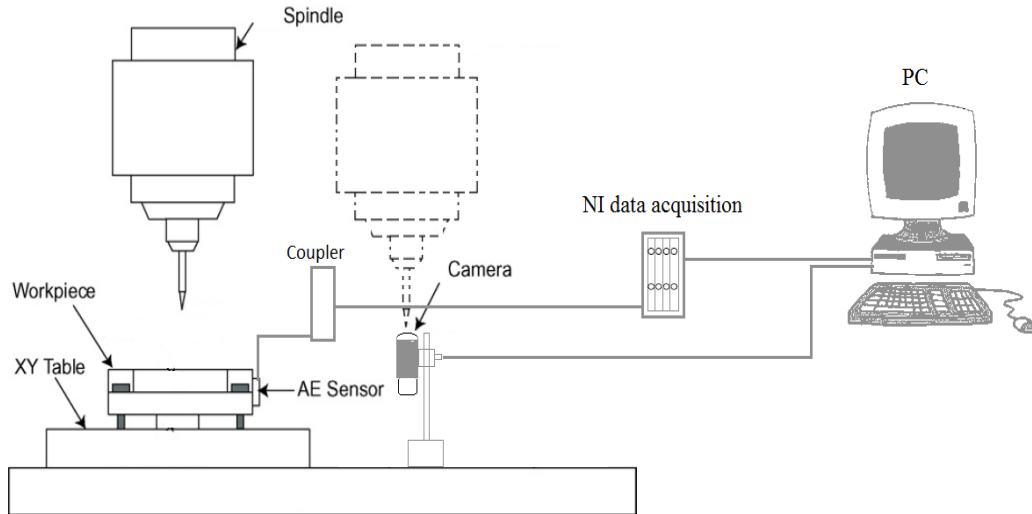


Figure 1. Experimental Setup

TOOL STATUS CATEGORIZATION

This study classified tool status according to tool life or tool wear, which is caused by progressive loss of tool material during cutting and which thus changes the shape of the cutting edge. Image J software was used to convert tool wear from a pixel scale to micrometer scale. Once the measuring scale was calibrated, tool wear was measured by counting pixels from the vision system and comparing the number with the scale on the reticle Figure 2.

The international organization for standardization [7] recommends that the tool be considered worn-out and reached its end point at 300 μm . Here, the output was assigned a value of 1 (for a fresh tool with wear less than 130 μm), 2 (for an average tool between 130 μm and 300 μm), or 3 (for a worn-out tool with wear greater than 300 μm). Figure 3 shows a fresh tool with 10 μm tool wear and Figure 4 shows a worn-out tool with 320 μm tool wear. In both cases, the tool has four flutes with a different level of wear, so the tool wear value represents an average.

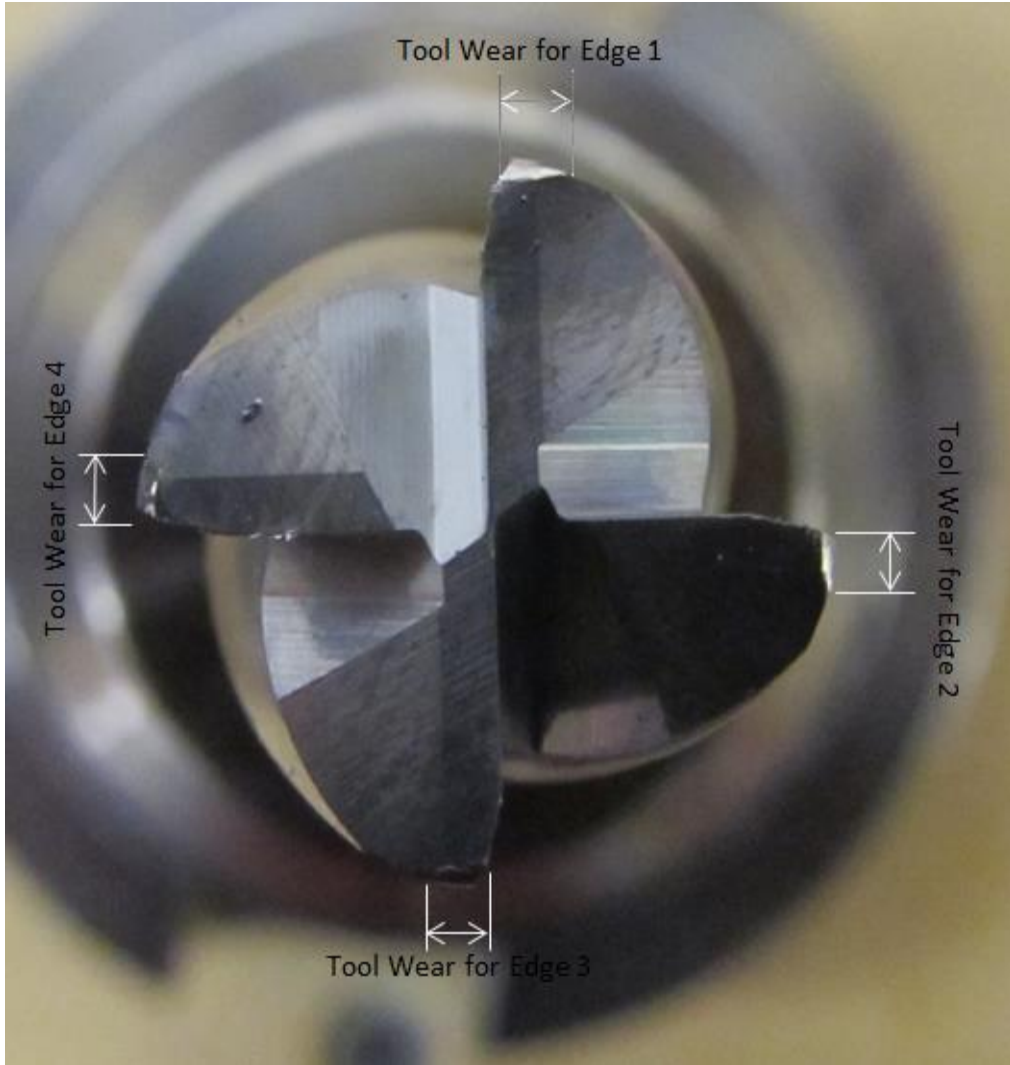
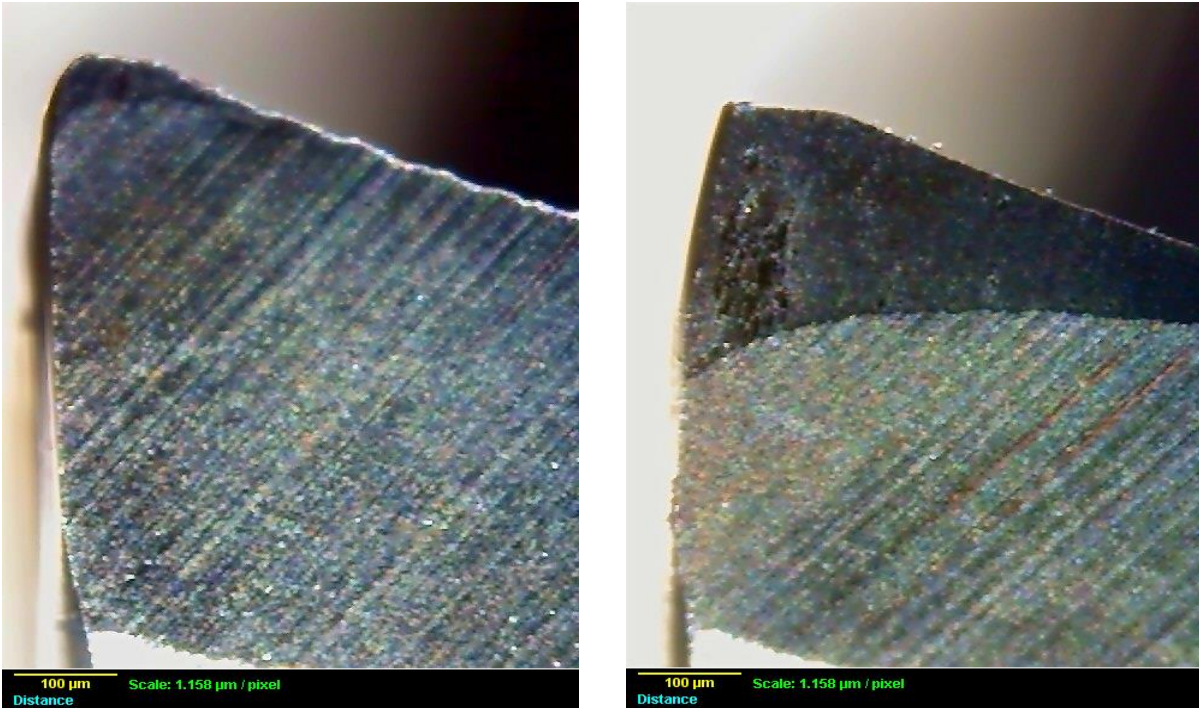


Figure 2. Tool Wear for 0.5 Inch End Mill



(a)

(b)

Figure 3. Tool Status (a) The Wear = 10 µm (b) The Wear = 320µm

DESIGN OF EXPERIMENTS

Most research has focused on the use of a force signal to detect, model, and control radial depth-of-cut and chip thickness [1-5], but this study used an acoustic emission sensor to predict axial depth-of-cut during end milling. The experiments described here were designed to use the most significant factors affecting the acoustic emission signal during the end milling process. Therefore, their outcomes are significant for the computation of depth-of-cut, and the model considers the cutting tool condition and the cutting variables. These factors include depth-of-cut, spindle speed, feed rate, and tool status.

A four factor-three level (3^4) full factorial experimental design with three replications, a total of 243 cutting tests were run randomly, and a range of cutting conditions were collected.

Table 1. Factors and Levels Defined for Experimentation

Depth of cut (mm)	Cutting Speed (RPM)	Feed Rate (mm/min)	Tool Status
0.5	1500	40	$\leq 130 \mu\text{m}$
1	3000	70	$> 130 \mu\text{m}$ and $\leq 300 \mu\text{m}$
2	5000	100	$> 300 \mu\text{m}$

PREDICTION USING ARTIFICIAL NEURAL NETWORK MODELING

Artificial neural network is statistical machine learning tool established based on the idea of how neurons in human brain work. The neural network consists of layers and nodes called neurons the number of layers and neurons depends on the difficulty of the problem being modeled. The input and output layers have neurons equal to the number of the inputs and the outputs respectively. The neurons connected by synapses which take a value from an input neuron and multiply it by specific weight and output the results, neurons have more complicated purpose, they add together all outputs from all synapses and apply activation function.

An artificial neural network at least has three layers; input layer, hidden layer, and output layer. If X is the input data vector which in this work is 1 by 4 vector Figure 4, $W(1)$ is weight matrix which is 4 by N matrix, where N is the number of neurons in the hidden layer, and $Z(2)$ is the transfer function of second layer.

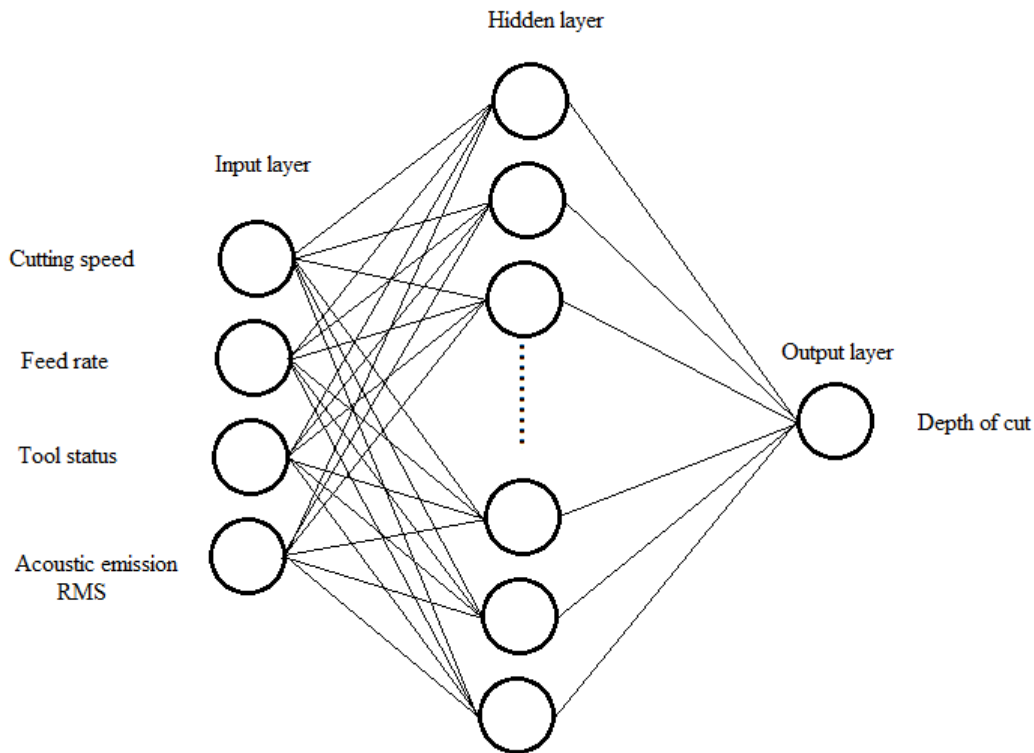


Figure 4. Neural Network Architecture

$$Z^{(2)} = X \times W^{(1)} \quad (1)$$

By applying transfer function to each element in $Z^{(2)}$, $a^{(2)}$ activation function of second layer can be obtained by

$$a^{(2)} = f(Z^{(2)}) \quad (2)$$

$a^{(2)}$ has the same size as $Z^{(2)}$. Now by multiplying weight matrix of second layer $W^{(2)}$ which is N by 1 matrix where there is only one output in our artificial neural network which is depth of cut

$$Z^{(3)} = a^{(2)} \times W^{(2)} \quad (3)$$

$Z^{(3)}$ is the transfer function of third layer. Finally activation function is applied to $Z^{(3)}$ in order to obtain the estimate for depth of cut y'

$$y' = f(Z^{(3)}) \quad (4)$$

Without training the network the estimation error will be very large, training is the process of updating the weight matrix to minimize the cost function J

$$J = \sum \frac{1}{2} (y - y')^2 \quad (5)$$

One of training algorithms can be used to train the ANN is a supervised learning algorithm called Backpropagation algorithm which adjust two parameters learning rate and momentum coefficient and keep them between 0 and 1. Equation 5 can be written as

$$J = \sum \frac{1}{2} (y - f(f(XW^{(1)})W^{(2)}))^2 \quad (6)$$

In order to save time and reduce calculations Gradient Descent method is used to guarantee searching for J in the correct direction and stop searching when smallest J is reached (cost function stops decreasing) by taken the partial derivative of J with respect of W ($\frac{\partial J}{\partial W}$), when $\frac{\partial J}{\partial W}$ is positive then the cost function is increasing and vice versa. This method is useful especially in multi-dimensional problems. Gradient descent can be performed either after using of all training data (batch gradient descent) or after each input–output pair (sequential gradient descent).

The neural network was trained with 147 data points (cutting conditions) to estimate the weights (includes biases) of candidate designs, and 48 data points was used to estimate the non-training performance error of candidate designs and also used to stop training once the non-training validation error estimate stops decreasing. Also 48 data points was used as testing data to obtain an unbiased estimate for the predicted error of unseen non-training data. Training, validation, and testing data were randomly chosen from different cutting conditions from the data set consists of 243 data points (cutting conditions).

Figure 5 illustrates the mean square error versus iteration (Epochs) number, while using the Bayesian regularization training algorithm. 25 neurons was used with in the hidden layer in this work. The network was trained for 90 iterations, at which time the performance was changing dramatically, the best performance was 1.81084 at epoch 65.

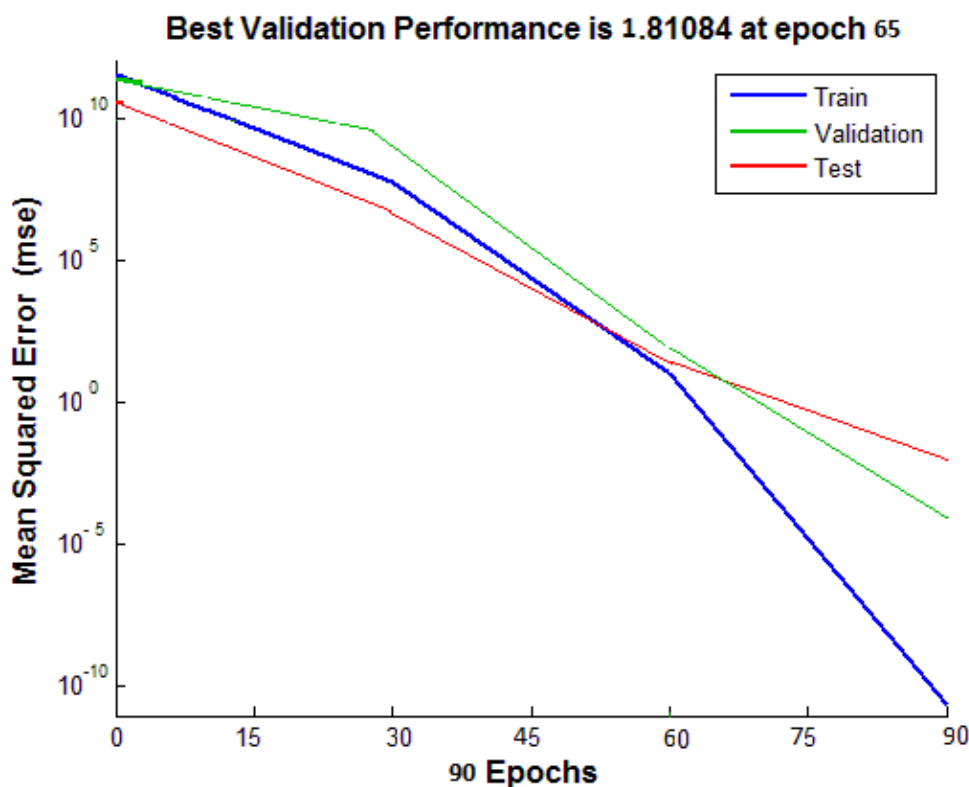


Figure 5. Neural network performance

ESTIMATION OF DEPTH-OF-CUT

Figure 6 shows the depth-of-cut estimated at 2 mm, 1 mm, and 0.5 mm with a feed rate of 40 mm/min and a cutting speed of 5000 rpm. Clearly, the system can detect the depth-of-cut with a maximum acceptable error. The accuracy of depth-of-cut estimation depends on the quality of the acquired signal.

This work tested the efficiency of the model in estimating depth-of-cut in an interrupted cutting process. As shown in Figure 7, a 25.2 mm slot was made in the workpiece perpendicular to the machining direction. The depth-of-cut was 1 mm, the cutting speed was 4000 rpm, the feed rate was 30 mm/min, and the tool was fresh. 51 second is the time required for the tool to cross the gap ($25.2/30$), and 25 second is both engagement and disengagement time subtracted from 51 seconds. Figure 8 shows that the model is able to distinguish the slot; thus the system is capable of detecting the engagement and the disengagement of the tool with the workpiece as well as the depth-of-cut.

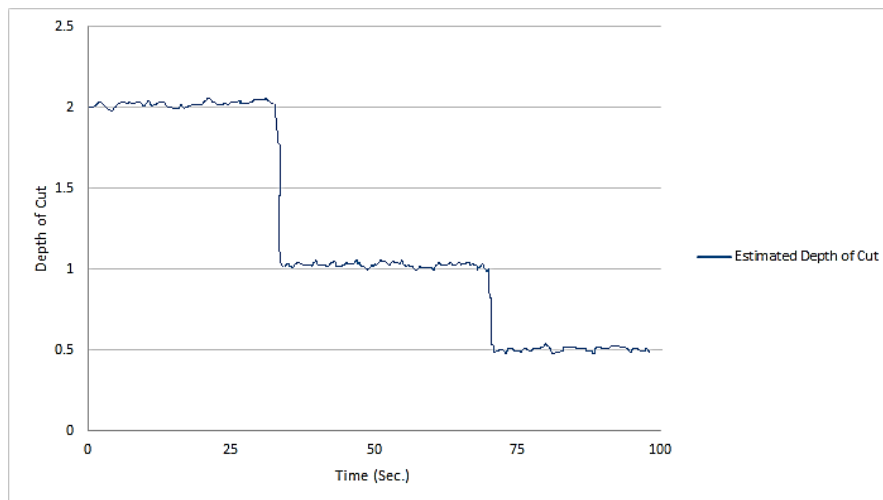
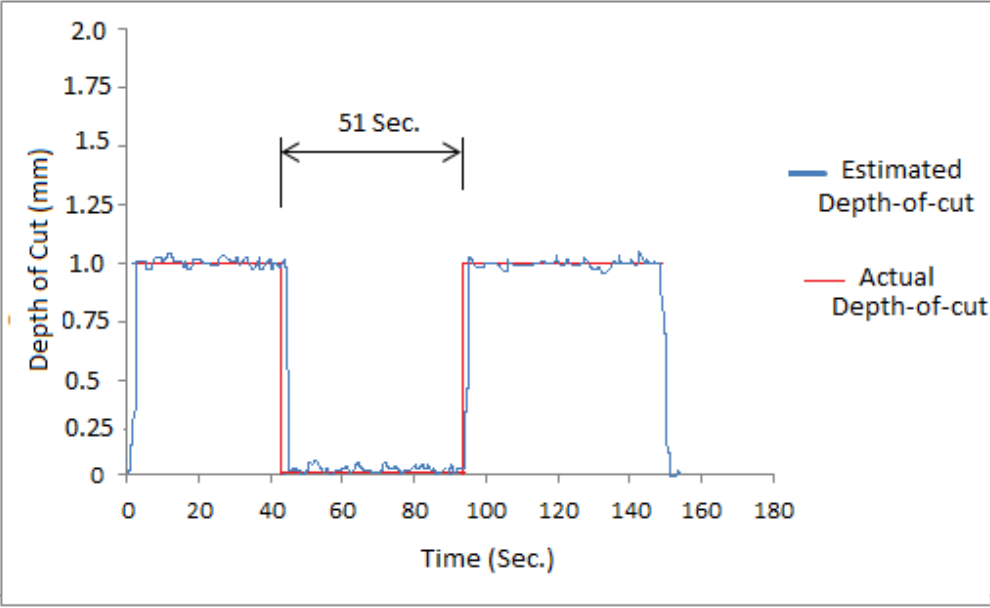
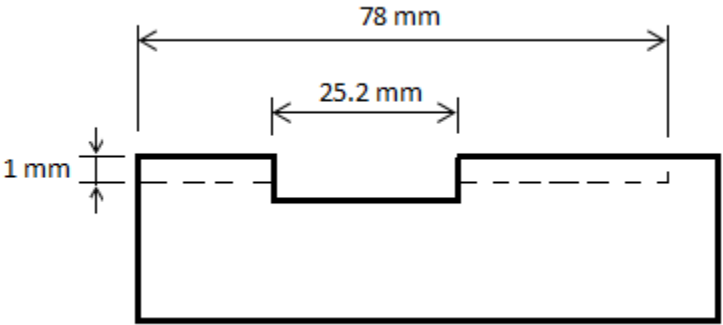


Figure 6. Shows the depth-of-cut estimated at 2 mm, 1 mm, and 0.5 mm with a feed rate of 40 mm/min and a cutting speed of 5000 rpm

Figure 8 shows both the nominal and estimated depth of cut for inclined surface cutting. A 10 mm ramp was created at the end of 60 mm cutting with 2 mm height as shown in the cutting geometry in the figure. The cutting speed was 4000 rpm, the feed rate was 30 mm/min, and the tool was fresh.

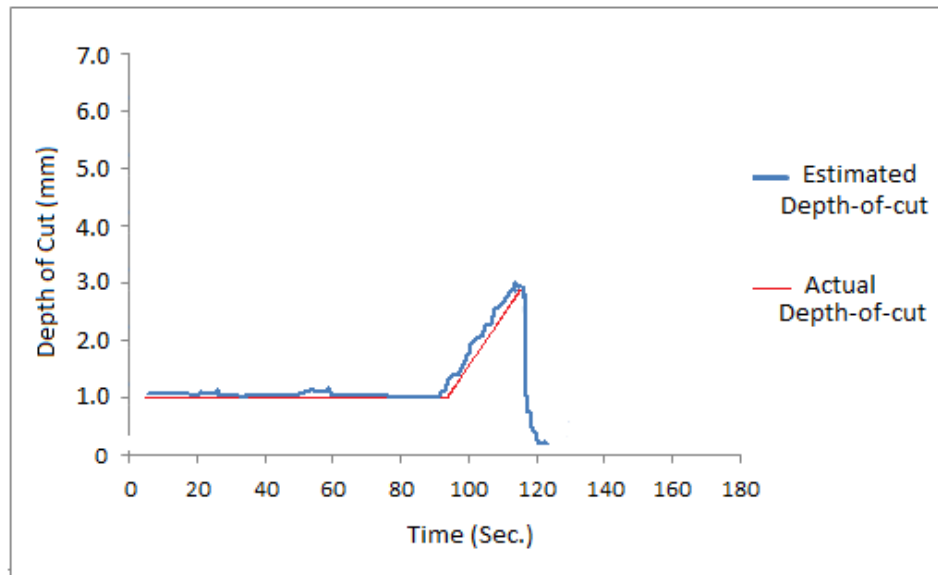


(a)

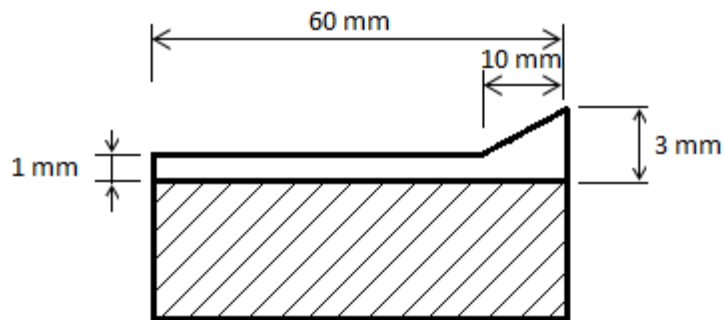


(b)

Figure 7. Interrupted Cutting (a) Nominal Depth-of-cut of 1 mm and Estimated Depth-of-cut (b) Schematic Representation of Cutting Geometry



(a)



(b)

Figure 8. Inclined Surface Cutting (a) Shows both the Nominal and Estimated Depth-of-cut for Inclined Surface Cutting (b) Schematic Representation of Cutting Geometry

As final test for the efficiency of the depth-of-cut detecting system, a free form surface was made from stainless steel 316 using laser deposition. The deposited part was first scanned using a 3D scanner, then the part was machined and scanned again as shown in figure 9.

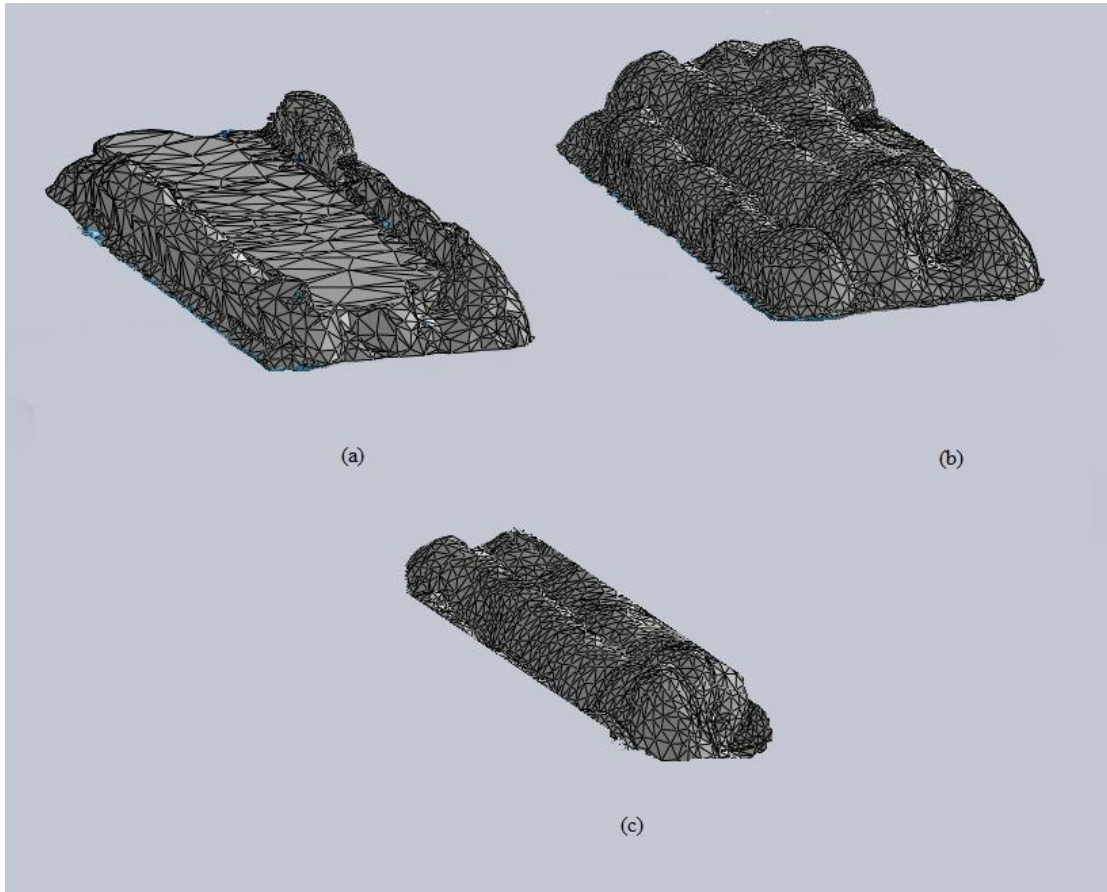


Figure 9. Scanned Deposited Material (a) Machined (b) Original (c) Removed

The difference between the two scans is the machined material. The machined material was sliced to fifty sections as shown in figure 10 and the area of each section was calculated. In order to calculate the depth-of-cut, the area of each section was divided by the tool diameter (12.7 mm).

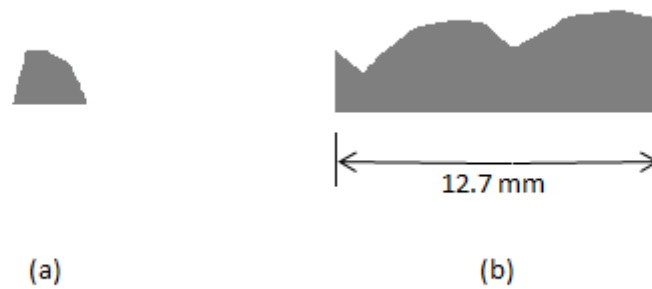


Figure 10. The Difference between the Laser Scans of Deposited Part and Machined Part
 (a) First Section of Removed Material. (b) Fifteenth Section of Removed Material.

Figure 11 shows the measured depth-of-cut from the sections and detected depth-of-cut by the acoustic emission sensor. The feed rate was 60 mm/min, cutting speed 4000 rpm, cutting length about 52 mm and the tool was worn-out. There is some deference between the measured and detected depth-of-cut in several points. This error might be caused by the change in the shear strength of the deposited material where the depth-of-cut detection model was made with material deposited at 800 W laser energy and the material tested now was made at 1000 W laser energy.

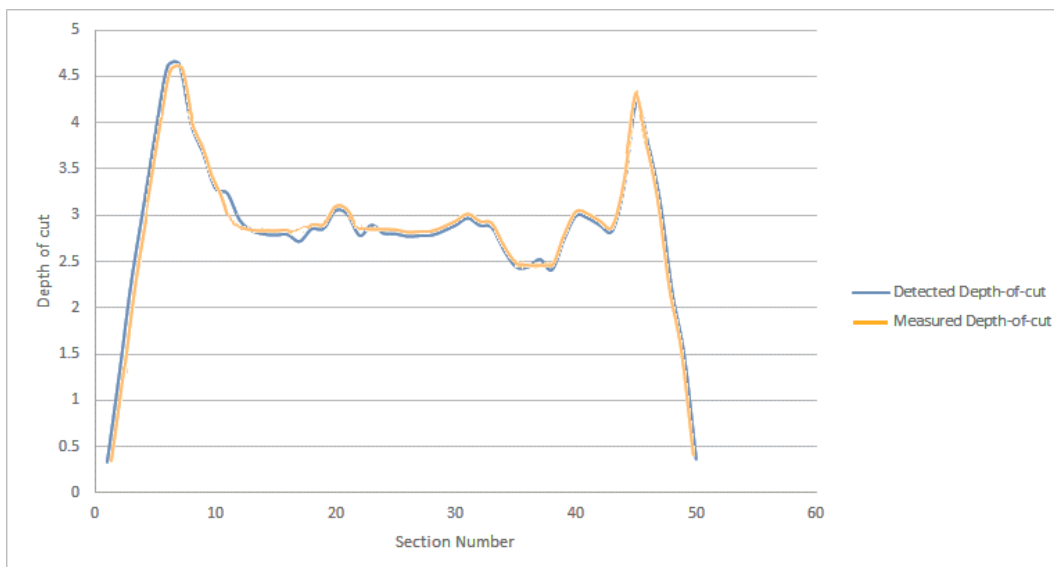


Figure 11. Measured Depth-of-cut from the Sections and Detected Depth-of-cut for a Deposited Material Detected by the Acoustic Emission Sensor

CONCLUSIONS

This research investigated experimentally the depth-of-cut and the acoustic emission variations during end-milling of deposited stainless steel 316 with an uncoated tungsten carbide tool under dry conditions, and it studied the correlation between the acoustic emission variation and the depth-of-cut. A full factorial experimental design was used to conduct experiments. As a result of this work, neural network model was developed to predict depth-of-cut in end milling.

The experimentally determined depth-of-cut values were compared with values predicted by the model, and the model is proved to be capable of predicting depth-of-cut with the acceptable margin of error. The results indicate that this model is robust and accurate. This study provides a depth-of-cut monitoring system for more efficient manufacturing in the future.

The Bayesian regularization training algorithm was used to train the network. 25 neurons was used with in the hidden layer in this work, the results obtained after training showed the effectiveness of this approach.

The model confirmed the effectiveness of estimating depth-of-cut for inclined surface cutting. The model is capable to distinguish the slot in an interrupted cutting process; therefore the system is capable of detecting the engagement and the disengagement of the tool with the workpiece as well as the depth-of-cut.

The main concern of this work was to detect the depth-of-cut for part made with Laser Metal Deposition, the model showed good agreement between measured depth-of-cut by using a 3D scanner and the predicted depth-of-cut by the artificial neural network model.

Future work will investigate signal processing and feature extraction since the root mean square is provided by the coupler and there is no control on low-pass and high-pass filters. A raw signal can be acquired from the sensor, and this signal contains more information than the root mean square signal, which was already processed inside the coupler. Also, the neural network approach can also be used to estimate feed rate, cutting speed or tool wear when the other cutting parameters are given.

References

- [1] Choi J. G., and Yang, M. Y, "In-Process Prediction of Cutting Depths in End Milling," *Int. J. Mach. Tools Manuf.*, 39(5), pp. 705–721. [Inspec] [ISI] , 1999
- [2] Yang Liuqing, DeVor Richard, Kapoor Shiv, "Analysis of Force Shape Characteristics and Detection of Depth-of-Cut Variations in End Milling," *J. Manuf. Sci. Eng.* 127, 454 , DOI:10.1115/1.1947207, 2005.
- [3] Wan M., W.H. Zhang, "Efficient algorithms for calculations of static form errors in peripheral milling," *Journal of Materials Processing Technology* 171, 156–165, 2006.
- [4] Li, H., and Shin, Y. C., "A Time-domain Dynamic Model for Chatter Prediction of Cylindrical Plunge Grinding Processes," *ASME J. Manuf. Sci. Eng.*, (in press), 2006.
- [5] Yonggang Kang, Wang Zhongqi, Wu Jianjun, and Jiang Chengyu, "Numerical prediction of static form errors in the end milling of thin-walled workpiece," *IET Conf. Pub.* 816, DOI:10.1049/cp:20060872, 2006.
- [6] Prickett, Paul, Siddiqui, Raees, Grosvenor, Roger , "The development of an end-milling process depth of cut monitoring system," *The International Journal of Advanced Manufacturing Technology*, 10.1007/s00170-010-2711-6, 2010.
- [7] ISO 8688-2, (1989). *Tool Life Testing in Milling – Part 2: End Milling*. International Standard, first edition.